Cell, Vol. 91, 649–659, November 28, 1997, Copyright ©1997 by Cell Press

Tumor Suppression at the Mouse *INK4a* Locus Mediated by the Alternative Reading Frame Product p19^{ARF}

Takehiko Kamijo,[1,2] Frederique Zindy,[2] Martine F. Roussel,[2] Dawn E. Quelle,[2,6] James R. Downing,[2,3] Richard A. Ashmun,[2,4] Gerard Grosveld,[5] and Charles J. Sherr[1,2,7]

[1] Howard Hughes Medical Institute
[2] Department of Tumor Cell Biology
[3] Department of Pathology and Laboratory Medicine
[4] Department of Experimental Oncology
[5] Department of Genetics
St. Jude Children's Research Hospital
332 North Lauderdale
Memphis, Tennessee 38105

Summary

The *INK4a* tumor suppressor locus encodes p16^{INK4a}, an inhibitor of cyclin D-dependent kinases, and p19^{ARF}, an alternative reading frame protein that also blocks cell proliferation. Surprisingly, mice lacking p19^{ARF} but expressing functional p16^{INK4a} develop tumors early in life. Their embryo fibroblasts (MEFs) do not senesce and are transformed by oncogenic Ha-*ras* alone. Conversion of *ARF*$^{+/+}$ or *ARF*$^{+/-}$ MEF strains to continuously proliferating cell lines involves loss of either p19^{ARF} or p53. p53-mediated checkpoint control is unperturbed in *ARF*-null fibroblast strains, whereas p53-negative cell lines are resistant to p19^{ARF}-induced growth arrest. Therefore, *INK4a* encodes growth inhibitory proteins that act upstream of the retinoblastoma protein and p53. Mutations and deletions targeting this locus in cancer cells are unlikely to be functionally equivalent.

Introduction

The two most frequently inactivated tumor suppressor genes in human cancer, irrespective of tumor type, site, and patient age, are *p53* and *INK4a* (Hall and Peters, 1996; Hainaut et al., 1997). The *INK4a* locus encodes p16^{INK4a}, a specific inhibitor of the cyclin D–dependent kinases CDK4 and CDK6 (Serrano et al., 1993) that antagonizes their ability to phosphorylate the retinoblastoma protein (Rb) and so prevents exit from G1 phase. Genetic disruption of the p16^{INK4a}—cyclin D-dependent kinase—Rb pathway is a common event in the life history of cancer cells, and it is achieved either through inactivation of the tumor suppressors (p16^{INK4a}, Rb) or by uncontrolled overexpression of the proto-oncogenes (D-type cyclins, CDK4) (Hunter and Pines, 1994; Weinburg et al., 1995; Hall and Peters, 1996; Sherr et al., 1996). Concurrent inactivation of p53 function inhibits such cells from arresting in G1 phase following DNA damage, decreases their genomic stability, and prevents them from undergoing apoptosis (Gottlieb and Oren, 1996; Ko and Prives, 1996; Levine, 1997), thereby collaborating with Rb loss of function in tumor cell progression.

A complication stems from the fact that the *INK4a* locus encodes a second alternative reading frame (ARF) protein whose enforced expression can also induce cell cycle arrest (Quelle et al., 1995b). While p16^{INK4a} is specified by three exons (designated 1α, 2, and 3), an alternative first exon (1β) maps ~13 kb 5′ to exon 1α in the mouse genome, and its coding sequences are spliced to the identical acceptor site of *INK4a* exon 2. The resulting mRNA specifies a p19^{ARF} protein of 169 amino acids, 65 encoded by exon 1β and the remainder by a second reading frame in exon 2. p19^{ARF} shares no amino acid homology with p16^{INK4a} or other known proteins, and apart from being a highly basic protein that localizes to nuclear speckles during interphase, its function remains unknown. Unlike p16^{INK4a}, p19^{ARF} overexpression induces both G1 and G2 phase arrest in rodent fibroblasts, whether or not the cells retain *INK4a*. The unusual organization of the *INK4a* locus is conserved in humans (Duro et al., 1995; Mao et al., 1995; Stone et al., 1995) and rats (Swafford et al., 1997), whereas three related but distinct *INK4* genes do not encode analogous ARF proteins.

Disruption of *INK4a* exon 2 in mice predisposes young animals to tumor development (Serrano et al., 1996). Their cultured mouse embryo fibroblasts (MEFs) fail to undergo a senescence crisis and can be transformed by oncogenic *ras* alleles, which, in the absence of collaborating "immortalizing oncogenes," would otherwise induce growth arrest (Lloyd et al., 1997; Serrano et al., 1997). Although it was clear that elimination of exon 2 of *INK4a* would compromise expression of both p16^{INK4a} and p19^{ARF}, it has been widely assumed that the observed phenotype stemmed from p16^{INK4a} disruption alone. We have now selectively disrupted *ARF* function in mice by deleting exon 1β and leaving all p16^{INK4a} coding sequences intact. Surprisingly, the previously described phenotypic consequences of *INK4a* disruption are reproduced in mice selectively nullizygous for p19^{ARF} alone, indicating that *ARF* is a bona fide tumor suppressor. Our results further suggest that *ARF* and *p53* regulate senescence of MEFs and that p19^{ARF} requires wild-type p53 to induce G1 phase arrest.

Results

Mice Lacking p19^{ARF} Express Wild-Type p16^{INK4a}

We used a conventional targeting vector to ablate *ARF* exon 1β in mouse embryonic stem cells, replacing it with a neomycin resistance (*neo*) gene (Figure 1A). Exon 1β is included within a 7.8 kb AflII fragment that was detected with a unique sequence genomic probe, but an AflII site inserted into the *neo* cassette reduced the size of the hybridizing fragment to 6 kb. Germline transmission of the mutant allele from a chimeric founder male and subsequent interbreeding of hemizygous offspring gave rise to normally developing animals lacking exon 1β at the expected Mendelian frequency (22% *ARF*-null, 52% heterozygous, 26% wild-type; total animals: 200) (Figure 1B). *INK4a* exon 1α and the tandemly linked *INK4b* locus remained intact (see below).

[6] Present address: Department of Pharmacology, University of Iowa College of Medicine, Iowa City, Iowa 52242-1109.
[7] To whom correspondence should be addressed.

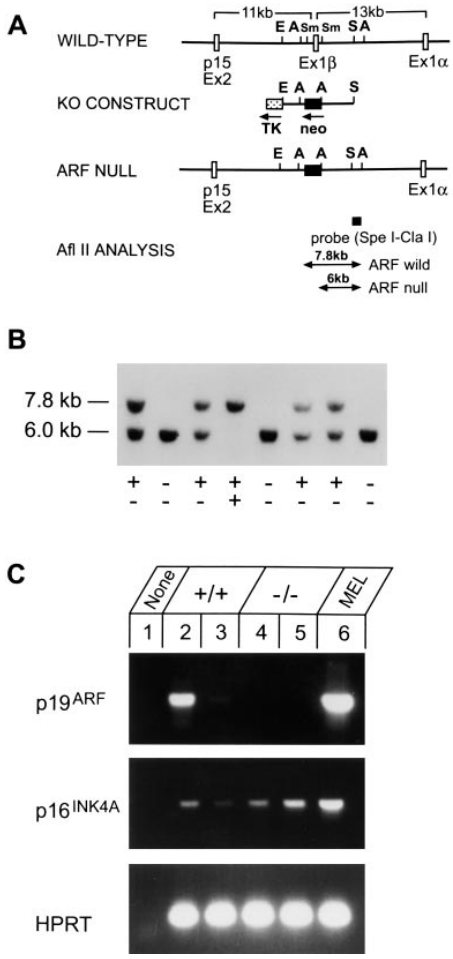

Figure 1. Loss of p19^{ARF} and Expression of p16^{INK4a} mRNA in ARF-Null Mice

(A) Schematic representation of the *INK4a* locus and *ARF* targeting vector. Open boxes denote exons with the 3′ end of *INK4b* to the left and the 5′ end of *INK4a* to the right. AflII sites (A) important for analysis of deletions are indicated, with the predicted sizes of the fragments containing intact exon 1β or *neo* noted below.

(B) Southern blot analysis of tail DNA from F2 animals with *ARF* genotype noted. The sizes of the AflII fragments predicted in (A) are indicated.

(C) RT-PCR amplification of RNA from the testis (lanes 2 and 4) and liver (lanes 3 and 5) of $ARF^{+/+}$ (lanes 2 and 3) and $-/-$ (lanes 4 and 5) mice. Lane 1 shows results with no templates, and lane 6 shows products recovered from equal amounts of MEL cell RNA used as a positive control. Amplification of hypoxanthyl phosphoribosyl transferase mRNA (HPRT) was used to demonstrate integrity of templates from all samples.

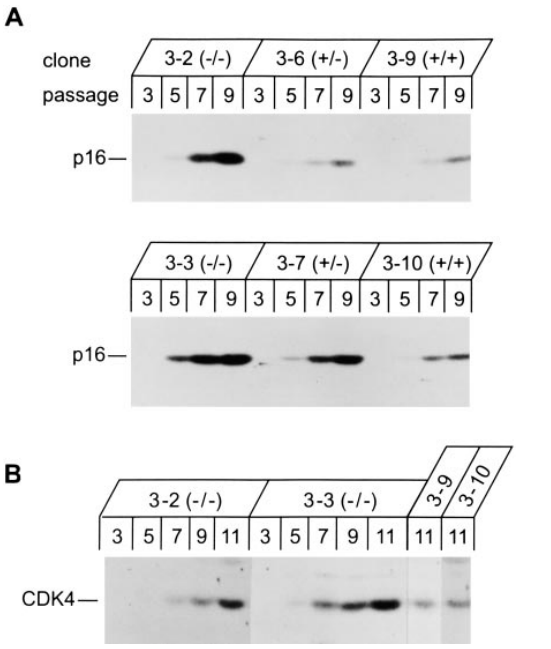

Figure 2. Expression of p16^{INK4a} in MEFs

(A) MEFs from six embryo strains were assayed at indicated passage numbers for p16^{INK4a} expression by sequential precipitation and immunoblotting with antiserum to the mouse p16 C terminus. Top and bottom panels were taken from parallel gels, shown with matched exposures. All precipitations were performed using an excess of titered antibody with equal protein inputs per sample.

(B) p16 immunoprecipitates as in (A) were separated on gels and blotted with antiserum directed to CDK4. Because p16 levels are relatively low in $ARF^{+/+}$ cells but increase as cells are passaged, results for coprecipitating CDK4 are shown with strains 3-9 and 3-10 at passage 11. Exposures in (A) and (B) are matched.

Animals lacking exon 1β (designated $ARF^{-/-}$) expressed transcripts encoding p16^{INK4a} but not p19^{ARF}. RT-PCR analysis showed that *ARF* β transcripts amplified from primers based on 5′ exon 1β and 3′ exon-2 sequences were expressed in testes and livers of $ARF^{+/+}$ animals (Figure 1C, lanes 2 and 3), but they were absent from their $ARF^{-/-}$ counterparts (lanes 4 and 5). Control murine erythroleukemia (MEL) cells expressed much higher levels of *ARF* RNA (lane 6). The levels of *ARF* mRNA in adult tissues are low, and the protein is not visualized with antiserum that detects the polypeptide in MEL cell lysates (Quelle et al., 1995b; Zindy et al., 1997). Authentic *INK4a* α transcripts containing 5′ exon 1α and 3′ exon-2 sequences were detected in both $ARF^{+/+}$ and $ARF^{-/-}$ animals (Figure 1C). Nucleotide sequencing of α transcripts amplified from testes of $ARF^{-/-}$ mice confirmed that they lacked mutations.

Neither p16^{INK4a} nor p19^{ARF} is expressed during mouse embryonic development, but when embryo cells are explanted into culture, p16^{INK4a} is induced and accumulates as MEFs are passaged (Zindy et al., 1997). MEF cultures initiated from genotyped embryos were passaged in vitro on a defined "3T9" schedule and tested for p16^{INK4a} expression. p16^{INK4a} was induced as six independent MEF cultures were passaged (Figure 2A), well before they underwent senescence and regardless of their *ARF* genotype. Even higher levels of p16^{INK4a} were detected in $ARF^{-/-}$ MEFs, as compared to those in cells retaining one or two wild-type *ARF* alleles. All inactivating p16^{INK4a} mutants described to date, including those that are temperature-sensitive, block the protein's ability to bind to CDK4 (Koh et al., 1995; Lukas et al., 1995; Ranade et al., 1995; Reymond and Brent, 1995; Wick et al., 1995; Yang et al., 1995; Parry and Peters, 1996; Quelle et al., 1997). Hence, the fact that p16^{INK4a} immunoprecipitates from $ARF^{-/-}$ MEFs contained CDK4 (Figure 2B) argues that the CDK inhibitor is functional. In proliferating MEFs, CDK4 levels exceed those of the *INK4* inhibitors, and as expected, assays for cyclin D– and CDK4-associated

Rb kinase activity confirmed the presence of catalytically active, cyclin D-bound pools of CDK4 in these cells (data not shown).

Early Passage MEFs Derived from *ARF*$^{-/-}$ Animals Are Impaired in Growth Control

Passaged *ARF*$^{+/+}$ cells initially underwent ~2 population doublings in the 3 days prior to dilution and replating, but their growth virtually ceased by passages 17–20 (Figure 3A). In contrast, cultures from *ARF*$^{-/-}$ embryos accumulated many more cells. At passage 5, they proliferated at significantly faster rates than their *ARF*$^{+/+}$ counterparts and grew to 3-fold higher densities at confluence (Figure 3B; note log scale on ordinate). *ARF*$^{+/-}$ cells showed an intermediate phenotype. By passage 10, the growth rates of *ARF*$^{+/+}$ and *ARF*$^{+/-}$ cells had further slowed; however, the division rate of *ARF*$^{-/-}$ cells was maintained (Figure 3B), and they proliferated continuously thereafter never undergoing a detectable senescence crisis (Figure 3A). Therefore, *ARF*$^{-/-}$ cells have an increased proliferative capacity, grow faster, and are somewhat less responsive to inhibition by cell-to-cell contact than their wild-type counterparts.

Another property of *INK4a* nullizygous MEFs is their capacity to be directly transformed by oncogenic *ras* alleles without a further requirement for collaborating "immortalizing genes," such as *E1a* or *myc* (Serrano et al., 1996; Weinberg, 1997). When early passage MEFs were transfected with an expression vector encoding oncogenic Ha-*ras* (Val-12), foci of transformed cells were detected in *ARF*$^{-/-}$ but not *ARF*$^{+/+}$ MEFs. We obtained 16 ± 12 foci per 60 mm diameter plate in 3 separate experiments with two different *ARF*$^{-/-}$ clones; these frequencies were similar to those obtained with *ARF*$^{+/+}$ MEFs transfected with vectors encoding both Ha-*ras* and *myc*. Morphologically transformed cells were highly refractile and no longer contact-inhibited (Figures 3Ca and 3Cb). Individually expanded transformed foci expressed p16^{INK4a} that coprecipitated with CDK4 (Figure 3Cc). Early passage *ARF*$^{-/-}$ cultures yielded no cells that were capable of anchorage-independent growth in semisolid medium, but *ras*-transformed subclones formed colonies in agar and tumors in SCID mice. When individual agar colonies picked at random were expanded, 12 of 12 continued to express p16^{INK4a} (data not shown). Thus, Ha-*ras* alone can oncogenically transform p19^{ARF}-negative, p16^{INK4a}-positive MEFs.

ARF or p53 Loss of Function in MEF Cell Lines

Rare MEF variants that weather the senescence crisis can become established as permanent cell lines (Todaro and Green, 1963), and these frequently contain mutant *p53* alleles (Harvey and Levine, 1991; Rittling and Denhardt, 1992) or sustain *INK4a* deletions (Kamb et al., 1994; Nobori et al., 1994; Zindy et al., 1997). In an experiment performed with four wild-type *ARF*$^{+/+}$ MEF strains, precrisis cells at passage 6 expressed p16^{INK4a} but no detectable p19^{ARF} (Figure 4A, lanes 1–4). Lysates from early passage strains contained wild-type p53 precipitated with an antibody (PAb246) that does not react with mutant forms (Yewdell et al., 1986). After emergence from crisis, however, MEFs from three strains had sustained *p53* mutations, as determined by selective precipitation of p53 by an antibody (PAb240) that recognizes mutant p53s but not the native p53 conformation

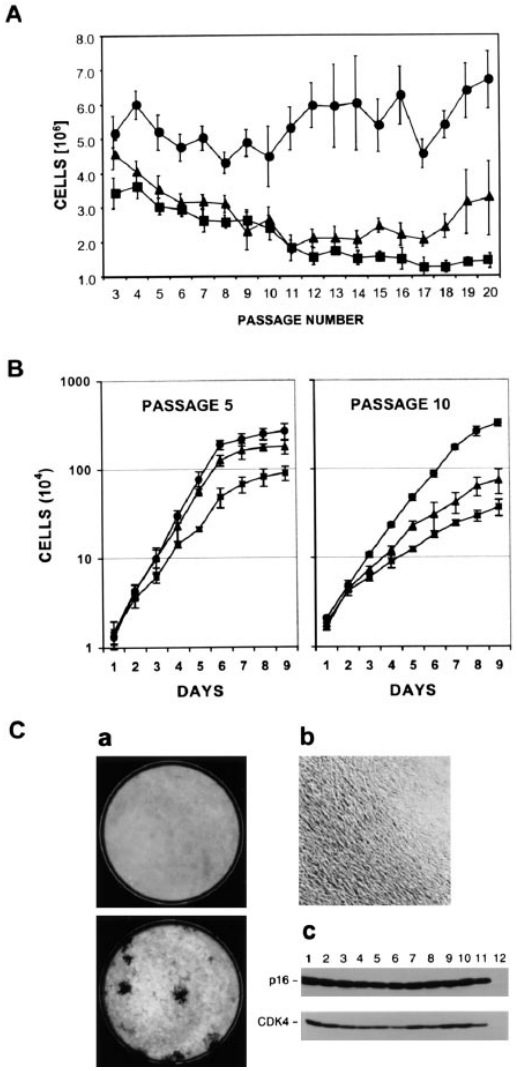

Figure 3. Kinetics of MEF Growth and *ras* Transformation

(A) Cell proliferation on a 3T9 protocol. At 3-day intervals, the total numbers of cells per culture (ordinate) were determined prior to redilution of the cells to 9×10^5 per 60 mm diameter dish for repassage. Data were pooled from 6–8 embryos of each genotype (total MEF strains = 20): *ARF*$^{-/-}$, circles; *ARF*$^{+/-}$, triangles; *ARF*$^{+/+}$, squares. Bars indicate standard errors from the mean.

(B) Cells from 3 *ARF*$^{-/-}$ (circles), 3 *ARF*$^{+/-}$ (triangles), and 3 *ARF*$^{+/+}$ (squares) MEF strains at passages 5 or 10 were seeded at 2×10^4 per culture in 20 replicate 60 mm diameter dishes. Duplicate dishes were harvested at daily intervals, and the total numbers of cells per culture (log scale ordinate) were determined. Data from different strains of the same genotype were pooled. Error bars indicate standard deviations (2σ) from the mean.

(C) MEF monolayer from *ARF*$^{-/-}$ cells transformed by *ras* versus a control plate transfected with the naked vector (a). Macroscopic foci of transformed cells (b) are heavily stained with Giemsa. In (c), lysates from 11 independently expanded foci (lanes 1–11) were precipitated with anti-p16^{INK4a}, transferred to nitrocellulose after electrophoresis on denaturing gels, and probed with the same antibody (top) or with antiserum to CDK4 (bottom) as indicated in the left margin. Lane 12 shows results with NIH-3T3 cells that lack the *INK4a* locus. Exposures are matched.

(Gannon et al., 1990) (lanes 5–7). Like MEL cells, which contain a disrupted *p53* gene, and others lacking functional p53 (Quelle et al., 1995b), these three MEF lines

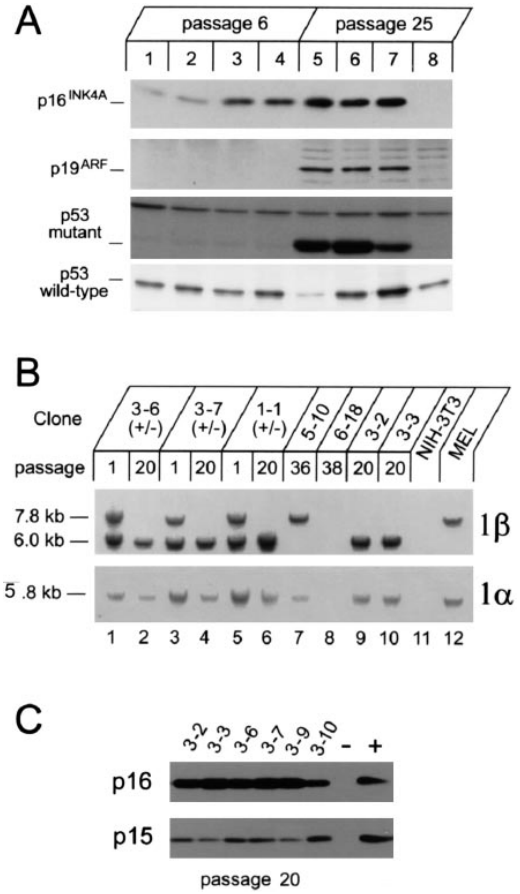

Figure 4. Expression of p16^{INK4a}, p19^{ARF}, and p53 in MEF Strains and Established Lines Derived from Them

(A) Expression of p16^{INK4a} and p19^{ARF} was documented by immunoprecipitation and immunoblotting, as in Figure 2. The same cells were metabolically labeled with [^{35}S]methionine and precipitated with monoclonal antibodies to wild-type or mutant p53 as indicated. Wild-type MEFs included clones 5-9 (lanes 1 and 5), 5-10 (lanes 2 and 6), 6-14 (lanes 3 and 7), and 6-18 (lanes 4 and 8). (B) Southern blot analysis of *ARF* exon 1β and *INK4a* exon 1α sequences. DNAs digested with AflII (top) or EcoRI (bottom) were hybridized with exon 1β genomic or exon 1α cDNA probes, respectively. Positions of diagnostic fragments containing (7.8 kb) or lacking (6.0 kb) exon 1β are indicated at the left of the top panel. Clones 3-6, 3-7, and 1-1 (lanes 1–6) were derived from mice hemizygous for *ARF* exon 1β. Clone 6-18 (lane 8) and NIH-3T3 cells (lane 11) originated from wild-type MEFs that sustained biallelic deletions of the entire *INK4a* locus, including intron sequences recognized by the probe. Clones 3-2 and 3-3 (lanes 9 and 10) were established from *ARF*-null animals that retained p16^{INK4a} coding sequences (Figure 2A). MEL cells (lane 12) do not express p53, and late passage clone 5-10 MEFs (lane 7) express a mutant form of the protein (A, lane b).

(C) MEFs at passage 20 were scored for INK4 protein expression by immunoblotting. Lysates from clone 6-18 and 5-10 cells were used as negative (−) and positive (+) controls.

synthesized abundant p19^{ARF} and even higher levels of p16^{INK4a} than those seen in early passage strains (lanes 5–7). In contrast, an established line that underwent deletion of both *INK4a* alleles expressed neither p16^{INK4a} nor p19^{ARF} and retained wild-type p53 (lane 8).

ARF$^{+/-}$ MEF strains generated established lines 4–6 passages earlier than *ARF*$^{+/+}$ cells (passages 18–20 in Figure 3A), preferentially yielding *ARF*$^{-/-}$ variants. Wild-type and mutant *ARF* alleles were detected with an exon 1β probe in MEFs from three such clones at passage 1, but only mutant *ARF* was detected at passage 20 when proliferating variants had emerged (Figure 4B). *ARF*$^{-/-}$ variants arising from *ARF*$^{+/-}$ MEF strains (lanes 2, 4, and 6), MEF lines from *ARF*-null mice (e.g., lanes 9 and 10), or cell lines arising from wild-type MEFs that sustained biallelic *ARF* deletions (lanes 8 and 11) synthesized only wild-type p53 (Figures 4B and 5, and data not shown). Conversely, cell lines that retained wild-type *ARF* alleles synthesized mutant p53 (e.g., Figure 4A, lanes 5–7; Figure 4B, lanes 7 and 12). Cell lines containing mutant p53 and retaining *ARF* rapidly became polyploid (cf. Harvey et al., 1993; Fukusawa et al., 1996), but all *ARF*$^{-/-}$/*p53*$^{+}$ lines remained pseudodiploid through additional passages (cf. Zindy et al., 1997; also clones 3-2 and 3-3 through passage 27). In short, functional loss of p53 or p19^{ARF} appeared to be mutually exclusive events as cells overcame a senescence block, with p53 predisposing to more rapid ploidy changes.

Although wild-type MEFs that sustained biallelic deletions of *ARF* lacked flanking *INK4a* and *INK4b* genes (Figure 4B, lanes 8 and 11), those containing a single *neo*-disrupted *ARF* allele gave rise to *ARF*$^{-/-}$ variants that retained *INK4a* (Figure 4B, lanes 1–6, exon 1α probe) and expressed both p16^{INK4a} and p15^{INK4b} (Figure 4C). These results strongly suggest that selection for *ARF* loss results in codeletion of *INK4a* and *INK4b* and not vice versa.

ARF-Induced Arrest Depends on p53

Levels of p19^{ARF} are elevated in cells lacking wild-type p53 function (Figure 1C, lane 6; Figure 4A, lanes 5–7) (Quelle et al., 1995b), which is compatible with the possibility that p53 may normally suppress *ARF*. However, we observed no change in p19^{ARF} levels when fibroblasts bearing a temperature-sensitive *p53* allele were shifted between permissive and nonpermissive temperatures, implying that p53 does not directly regulate *ARF* expression (Quelle et al., 1997).

Early passage MEFs, regardless of their *ARF* status, expressed equivalent levels of wild-type p53 (Figure 5A), which was rapidly and transiently induced in *ARF*-null cells in response to γ irradiation (Figure 5B). Levels of the p53-responsive CDK inhibitor, p21^{Cip1}, also rose within 2–4 hr of exposure to 5 Gy ionizing radiation (Figure 5B). To see whether *ARF*-null cells underwent G1 phase arrest in response to DNA damage, arrested serum-starved cultures from two different sets of *ARF*$^{-/-}$ and *ARF*$^{+/+}$ MEF strains were irradiated with 5 or 20 Gy and transferred into medium containing serum and BrdU. Cells were stained for DNA content (propidium iodide) and replicative DNA synthesis (BrdU) 24 hr after release from the G_0 block, and the S phase fractions were determined by flow cytometry. Although p53-negative MEFs are not inhibited from entering S phase after irradiation (Kastan et al., 1991; Kuerbitz et al., 1992; Deng et al., 1995), both *ARF*$^{+/+}$ and *ARF*$^{-/-}$ MEFs underwent G1 arrest at the same efficiency. The percentages of cells entering S phase after irradiation relative to unirradiated cells were 26% for *ARF*$^{+/+}$ and 30.9% for *ARF*$^{-/-}$ MEFs,

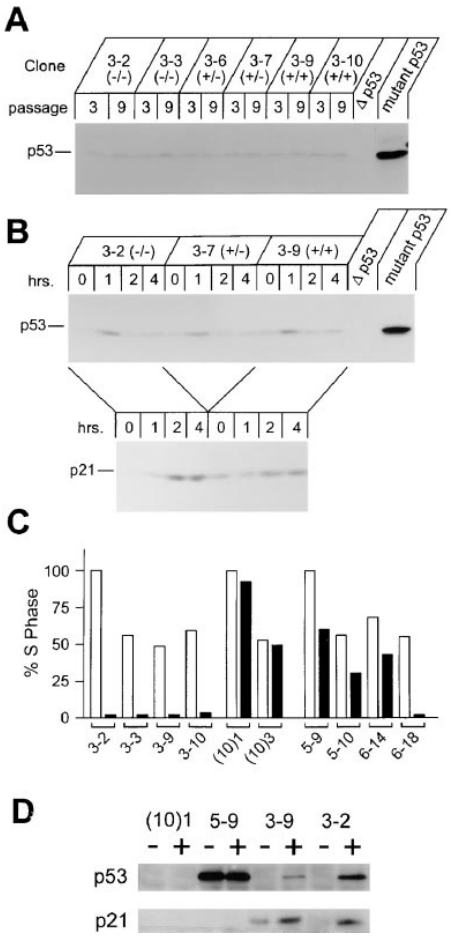

Figure 5. ARF and p53 Interactions in MEFs

(A) Lysates from MEFs with different *ARF* genotypes were analyzed for p53 status by immunoblotting with an antibody that recognizes both wild-type and mutant p53. No mutant p53 was detected by precipitation with PAb240, whereas the wild-type form was again detected with PAb246 (data not shown).

(B) Cells with the indicated *ARF* genotype were irradiated with 5 Gy, and p53 and p21 were measured by immunoblotting at the indicated times (hr) after exposure. Lysates of clone 5-10 cells were used to document higher levels of mutant p53 expression on a per protein basis. Balb-3T3 (10)1 cells null for p53 (Δp53) were used as a negative control.

(C) MEF strains (clones 3-2, 3-3, 3-9, and 3-10 at passage 9), established MEF cell lines (clones 5-9, 5-10, 6-14, and 6-18 at passage 26), and Balb-3T3 derivatives lacking p53 were infected with an ARF-retrovirus (closed bars) or with the naked control vector (open bars). Cells were labeled for 24 hr with [^{3}H]thymidine 48 hr postinfection. Results with MEF strains, Balb-3T3 derivatives, and established MEF lines were normalized to values (set to 100%) obtained with 3-2, 10-1, and 5-9 cells, respectively, infected with the control vector. Standard deviations (data not shown) were less than ±10% of the mean.

(D) Cells infected with ARF-retrovirus (+) or with vector alone (−) were lysed 24 hr postinfection, and gel-separated proteins were immunoblotted for p53 and p21.

versus >90% for p53-negative MEFs. Loss of growth control in $ARF^{-/-}$ cells is therefore due neither to *p53* mutation or deletion, nor to apparent perturbation of its G1 checkpoint function.

Both $ARF^{-/-}$ and $ARF^{+/+}$ MEFs at passage 9 were completely inhibited from entering S phase when tested 24 hr after infection with an ARF-coding retrovirus (Figure 5C). NIH-3T3 cells and clone 6-18 cells lacking the entire *INK4a* locus were also sensitive, underscoring the fact that arrest by $p19^{ARF}$ does not depend upon $p16^{INK4a}$. On the other hand, established (10)1 and (10)3 Balb-3T3 cell lines lacking p53, and cell lines established from $ARF^{+/+}$ MEFs that had sustained p53 mutations, were resistant to growth arrest by vectors encoding $p19^{ARF}$ (Figure 5C). The latter cells expressed elevated levels of endogenous $p19^{ARF}$ (e.g., Figure 4A, lanes 5–7) that closely approximated those achieved in vector-infected $p53^{+}$/*ARF*-null clones (Quelle et al., 1995b). In summary, 7 of 7 tested cell lines lacking p53 function lost responsiveness to $p19^{ARF}$, while 4 of 4 $p53^{+}$/*ARF*-null lines were sensitive.

Although basal p53 levels were similar in $ARF^{-/-}$ and $ARF^{+/+}$ cells (Figure 5A), *ARF*-null MEFs reproducibly expressed lower levels of $p21^{Cip1}$ (e.g., Figure 5B, 0 hr). In cells infected with retroviral vectors encoding $p19^{ARF}$, p53 and $p21^{Cip1}$ were induced in clones expressing wild-type p53, regardless of their *ARF* genotype (Figure 5D). In contrast, cells lacking p53 [clone 10(1)] or containing mutant p53 (5-9) exhibited no $p19^{ARF}$-dependent induction of $p21^{Cip1}$; these observations were reproduced in lines 10(3), 5-10, and 6-14. Therefore, ectopic expression of $p19^{ARF}$ increases $p21^{Cip1}$ expression in a p53-dependent manner.

$p19^{ARF}$-Deficient Mice Develop Cancer

By 2 months of age, $ARF^{-/-}$ mice began to develop tumors spontaneously (Table 1). Six of 18 *ARF*-null animals exhibited malignant tumors by six months of age, but none were observed in 23 $ARF^{+/+}$ or 66 $ARF^{+/-}$ mice during the same period. Nine of 11 $ARF^{-/-}$ mice treated one week after birth with DMBA developed tumors by 9–20 weeks of age (Table 1). Skin tumors occurred at multiple sites and exhibited varying degrees of anaplasia, with two mice manifesting invasive, poorly differentiated epidermoid carcinomas. Three animals within this group developed two tumors of completely different histologic types. Identically treated control animals (12 $ARF^{+/+}$ and 13 $ARF^{+/-}$) did not develop tumors during the six-month observation period. DMBA treatment predisposes to development of skin tumors under the conditions used, but other control animals derived from the same mouse strains did not develop skin tumors after DMBA treatment until they were over 10 months old, consistent with historical data (Reiners, et al., 1984; Naito and DiGiovanni, 1989). Four of six mice that were γ-irradiated as newborns developed fibrosarcomas or anaplastic T cell lymphomas.

Enough tumor tissue was obtained from six mice (Table 1) to demonstrate $p16^{INK4a}$-coding transcripts (Figure 6A) and protein (Figure 6B) in uncultured cells. Fibrosarcoma cells explanted into culture from animal K5 grew rapidly and were maintained as a continuously proliferating cell line. Like the primary tumor, these synthesized $p16^{INK4a}$ mRNA and protein. The lymphoma from mouse K90 also synthesized $p16^{INK4a}$. Both the K5 and K90 tumor cells expressed $p16^{INK4a}$-associated CDK4, again implying that the CDK inhibitor was functionally

Table 1. Tumors in Young ARF-Null Mice

Mouse	Sex	Age (weeks)	Treatment	Histology	p16 PCR	p16 Blot
K5	M	18	None	Fibrosarcoma	+*	+
K11	M	8	None	Metastatic salivary gland carcinoma	+*	+
K17	F	21	None	Thymoma	ND	ND
K75	F	11	None	Malignant fibrous histiocytoma	ND	ND
K116	M	18	None	Lymphoma (brain)	ND	ND
K199	M	16	None	Fibrosarcoma	ND	ND
K86	F	12	DMBA	Epidermal papilloma (4 sites)	ND	+
K88	F	20	DMBA	Epidermal papilloma	ND	ND
K90	F	14	DMBA	Lymphoma and epidermal papilloma	+	+
K98	F	13	DMBA	Metastatic epidermoid carcinoma	ND	+
K106	M	9	DMBA	Invasive epidermoid carcinoma	+*	+
K149	M	12	DMBA	Fibrosarcoma, malignant adenexal tumor	ND	ND
K150	M	14	DMBA	Epidermal papilloma (2 sites)	ND	ND
K151	F	13	DMBA	Fibrosarcoma and epidermal papilloma	ND	ND
K163	M	13	DMBA	Epidermal papilloma (4 sites)	ND	ND
K173	M	12	Irradiation	Fibrosarcoma	ND	ND
K175	M	12	Irradiation	Lymphoma	ND	ND
K178	F	13	Irradiation	Fibrosarcoma	ND	ND
K185	M	19	Irradiation	Lymphoma	ND	ND

Age refers to date of tumor detection or death of the animal. Where indicated, mice received ionizing radiation (4 Gy) (Kemp et al., 1994) or were treated with DMBA 5–7 days after birth (Serrano et al., 1996). Nine of 11 DMBA-treated animals, 4 of 6 animals that received sublethal γ-irradiation, and 6 of 18 untreated mice developed tumors by 5 months of age. Fibrosarcomas arose subcutaneously and were all highly invasive to skeletal muscle and bone. Skin tumors in DMBA-treated animals exhibited variable degrees of anaplasia, with lower grade papillomatous growths sometimes arising at multiple independent sites, and with higher grade carcinomas presenting as either locally invasive or frankly metastatic variants. Lymphomas were anaplastic large-cell type with T cell markers. Detection of $p16^{INK4a}$ transcripts (PCR) or protein (immunoblotting) in primary tumor tissues is noted by (+); not done is noted by "N.D."; and RT-PCR products taken for nucleotide sequencing are noted by (*).

wild-type (Figure 6B). Similar protein data were obtained with four other primary tumors (animals K11, K86, K98, K106). Nucleotide sequencing analysis of PCR products confirmed that $p16^{INK4a}$ transcripts amplified from tumors taken from animals K5, K11, and K106 had not sustained mutations. We conclude that $p19^{ARF}$ functions as a bona fide tumor suppressor.

Discussion

$p16^{INK4a}$ Is Expressed Appropriately in Cells Lacking ARF

Mice lacking exon 2 of the *INK4a* gene were previously found to develop tumors of many histologic types (Serrano et al., 1996). MEFs derived from these animals became established in culture without undergoing a senescence crisis, and even cells in early passage could be transformed by oncogenic Ha-*ras* alone. Given that these previously reported features of *INK4a*-null animals have now been recapitulated in animals lacking only $p19^{ARF}$, the relative contributions of $p19^{ARF}$ and $p16^{INK4a}$ to tumor suppression need to be reevaluated.

A trivial interpretation of our results might have been that disruption of *ARF* exon 1β perturbed $p16^{INK4a}$ expression. However, normal tissues from $ARF^{-/-}$ mice, cultured MEFs, *ras*-transformed fibroblasts, mouse tumors, and cell lines derived from them all expressed $p16^{INK4a}$. The hallmark of nonfunctional $p16^{INK4a}$ point mutants tested so far, including several temperature-sensitive alleles, is their inability to bind to CDK4 or CDK6; thus, the simplest and most reliable assay for $p16^{INK4a}$ function is its physical interaction with these catalytic subunits (Parry and Peters, 1996). By this criterion, $p16^{INK4a}$ in tissues of *ARF*-nullizygous mice and in cultured cells and tumors derived from them, was functionally wild type. Nucleotide sequencing of RT-PCR products from testes and from several primary tumors confirmed this prediction. Although we do not preclude that $p16^{INK4a}$ might undergo mutation in *ARF*-null animals, the observed results clearly do not reflect such a mechanism.

Typical patterns of $p16^{INK4a}$ and $p15^{INK4b}$ expression were maintained in MEFs, irrespective of whether or not they retained *ARF*. In fact, $p16^{INK4a}$ protein levels were higher in $ARF^{-/-}$ MEFs than in their matched $ARF^{+/-}$ and $ARF^{+/+}$ counterparts, possibly because without competition from the upstream *ARF* β promoter, α transcripts encoding $p16^{INK4a}$ may be more efficiently spliced. Thus, insertion of *neo* into exon 1β did not dampen expression from the two flanking *INK4* genes. The fact that *ARF*-null MEFs did not exhibit a detectable senescence crisis fingers $p19^{ARF}$ rather than $p16^{INK4a}$ as the mediator of these events. When wild-type MEFs underwent biallelic deletion of *ARF* during establishment, the *INK4a* and *INK4b* genes were concomitantly lost. However, *ARF*-null cell lines arising from $ARF^{+/-}$ MEF strains retained hemizygous *INK4* coding sequences and continued to express $p16^{INK4a}$ and $p15^{INK4b}$, implying that *INK4a* and *INK4b* deletions occur as a consequence of selection for cells that bypass the senescence block. $ARF^{-/-}$ cells transformed by Ha-*ras* (Val-12) alone continued to express functional $p16^{INK4a}$, so the loss of $p19^{ARF}$ mimics effects of "immortalizing genes" such as E1a and *myc* that can similarly collaborate with *ras* (Weinberg, 1997).

ARF Functionally Interacts with p53

Expression of $p19^{ARF}$ was not detected in early passage wild-type MEF strains, but it was readily observed in

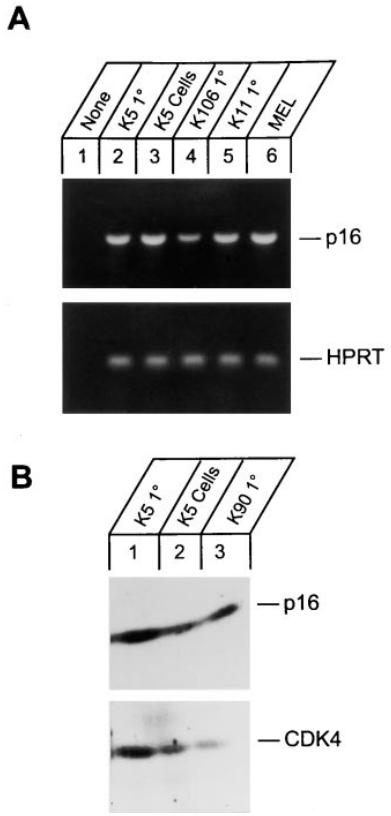

Figure 6. Expression of p16^{INK4a} in Mouse Tumors

(A) RT–PCR analysis of tumor tissue. Total mRNAs extracted directly from the K5 fibrosarcoma (1°), a cell line established from it (K5 cells), and one directly from the K11 lymphoma (1°) were amplified using p16 and HPRT primers as in Figure 1C. Lanes 1 and 6 show results with no template and MEL cell mRNA, respectively.

(B) Cell lysates (800 μg protein per lane) from the K5 and K90 primary tumors (1°) and from the established K5 cell line were precipitated with antibodies to the p16^{INK4a} C terminus, and proteins separated on denaturing gels were blotted with the same antibody (top) or with rabbit antiserum to CDK4 (bottom).

derived cell lines containing mutant p53. We have only negative evidence that p53 directly regulates p19^{ARF} expression in fibroblasts (Quelle et al., 1997); therefore, significantly higher levels of endogenous p19^{ARF} observed in cells lacking p53 function might instead reflect selection for p53 loss in cells in which p19^{ARF} had already been induced. *ARF*-positive MEFs that weather a senescence crisis and retain the gene likely become established as a result of independent mechanisms that override p19^{ARF}-mediated growth suppression, and two lines of evidence suggest that loss of p53 function is the key event. First, cells lacking a functional *p53* gene are resistant to p19^{ARF}-induced cell cycle arrest. Second, established MEF lines that retained *ARF* sustained p53 mutations, whereas those that deleted *ARF* preserved p53 function. Lines with mutant p53 rapidly become polyploid (Levine, 1997), whereas *ARF*-null lines that retain p53 function seem to remain pseudodiploid through more passages. In mice then, *p53* and *ARF* inactivation appear to represent alternative mechanisms for bypassing the senescence block, and p53 loss predisposes more strongly to changes in ploidy (Fukusawa et al., 1996). Species with longer life spans likely manifest more stringent controls over cell senescence, and in cultures of human cells, loss of both *p53* and *ARF*, or other collaborating events, may well be required to endow them with an extended proliferative capacity (Rogan et al., 1995; Alcorta et al., 1996; Hara et al., 1996; Noble et al., 1996; Reznikoff et al., 1996; Serrano et al., 1997).

Neither point mutations within *ARF* exon 1β nor promoter hypermethylation have so far been detected in tumors or in tumor-derived cell lines (Mao et al., 1995; Merlo et al., 1995; Shapiro et al., 1995; Stone et al., 1995; Fitzgerald et al., 1996; Herzog et al., 1996; Kubo et al., 1997; Swafford et al., 1997; Tanaka et al., 1997). Consequently, *ARF* inactivation may require biallelic deletions, as opposed to p53, whose dominant-negative mutants subvert the function of the wild-type tetrameric product. During passage in culture, *ARF*$^{+/-}$ MEFs sustained deletions of their remaining *ARF* allele while retaining wild-type p53, and such strains became established as cell lines 4–6 passages earlier than *ARF*$^{+/+}$ cells. In normal MEFs containing two wild-type *ARF* alleles, p53 mutation is readily detected (Harvey and Levine, 1991), but in cells hemizygous for *ARF*, loss of the remaining wild-type *ARF* allele is at least as frequent an occurrence.

MEF cell lines lacking *ARF*, whether directly derived from nullizygous animals or from wild-type cells that had deleted both copies of the gene during the process of establishment, promptly stopped proliferating when infected with a retrovirus encoding p19^{ARF}. Both early and late passage *ARF*$^{-/-}$ MEFs expressed low levels of p53, which was induced by γ irradiation and, in turn, was able to induce p21^{Cip1} and to block cell proliferation. Thus, such cells were not defective in p53-mediated checkpoint control. In contrast, *ARF*-positive cell lines that acquired p53 mutations or deletions were refractory to p19^{ARF}-induced growth arrest. MEFs from *p53*-null mice are genetically unstable and do not senesce either (Harvey et al., 1993). In principle, p19^{ARF} might exert its effects through a p53-regulated gene such as p21^{Cip1}(El-Deiry et al., 1993), which was cloned as a senescent cell-derived growth inhibitor (Noda et al., 1994). In agreement with this hypothesis, basal p21^{Cip1} levels were reduced in *ARF*$^{-/-}$ versus *ARF*$^{+/+}$ MEFs, and enforced expression of p19^{ARF} induced p21^{Cip1} in a p53-dependent manner. Although induction of p53 and p21^{Cip1} by γ irradiation does not depend on *ARF*, enforced p19^{ARF} expression could conceivably trigger a stress response that mimics effects of DNA damage. Whatever the exact mechanisms, observations that p19^{ARF} can function "upstream" of p53 raise the possibility that the *INK4a/ARF* locus is a master growth regulator whose encoded proteins interface with both the Rb (p16^{INK4a}) and p53 (p19^{ARF}) pathways.

Despite the fact that p19^{ARF} depends on p53 for inducing growth arrest, loss of both proteins can occur in tumor cells. We found that a fibrosarcoma that arose spontaneously in an *ARF*$^{-/-}$ mouse had lost *p53* but retained wild-type p16^{INK4a}, indicating that p19^{ARF} and p53 can likely collaborate in tumor progression. One obvious possibility is that p53 can regulate apoptotic functions in *ARF*$^{-/-}$ cells unrelated to cell cycle progression per se.

p16^{INK4a} and Tumorigenesis?

Although it is evident that p19^{ARF} functions as a tumor suppressor in mice, contributions of p16^{INK4a} to the phenotype of *INK4a*-null animals are not excluded by our studies. We cannot readily compare the spectrum of tumors in *ARF*$^{-/-}$ mice with those observed by Serrano et al, 1996. We saw lymphomas and fibrosarcomas, which predominated in their studies (as in *p53*-null mice [Donehower et al., 1992; Jacks et al., 1994; Kemp et al., 1994]), as well as tumors which are otherwise very rare. The timing of tumor appearance was also similar. Our mice are still relatively young, and it will be necessary to examine and compare many more animals before reaching firm conclusions about the types and frequencies of tumors that arise in the two strains. Another ambiguity concerns the status of *ARF* mRNA expression in mice disrupted in *INK4a* exon 2 versus 1α. The amino-terminal domain of p19^{ARF} is necessary and sufficient to induce cell cycle arrest (Quelle et al., 1997), so animals disrupted in exon 2 may not be completely devoid of *ARF* function if stable mRNAs encoding exon 1β are translated. Ultimately, then, the extent to which p16^{INK4a} loss independently contributes to tumorigenesis in mice will require analysis of a *p16*−null/*ARF*-positive strain.

Data implicating p16^{INK4a} as a tumor suppressor in humans remains compelling. In certain tumor types, inactivating point mutations of p16^{INK4a} are common, whereas deletions are rare (Hirama and Koeffler, 1995; Hall and Peters, 1996; Pollock et al., 1996). Some mutations fall into exon 1α, which does not encode p19^{ARF} (Gruis et al., 1995; Holland et al., 1995; Walker et al., 1995), and the missense mutations within exon 2 that affect both reading frames can selectively target p16^{INK4a} (Quelle et al., 1997). Therefore, cancer−specific point mutations preferentially, and perhaps exclusively, impinge on p16^{INK4a}. If the mouse models have any predictive value for human cancer, *INK4a* deletions and mutations must be functionally distinct.

Experimental Procedures

Targeting Vector

Bacteriophages containing *ARF* exon 1β were isolated from a 129/SvjE mouse genomic library (Van Deursen et al., 1995) using p19^{ARF}-specific cDNA probes (Quelle et al., 1995b). Restriction enzyme maps of the *INK4a* and *INK4b* loci were determined using bacterial artificial chromosome (BAC) clones (Genome Systems, St. Louis, MO). To construct the targeting vector, a 1 kb SmaI fragment containing Exon 1β was deleted and replaced with a *neo* cassette flanked by 2.5 kb EcoRI (E) to SmaI (Sm) and 5 kb SmaI to SpeI (S) fragments derived from the *ARF* locus; screening of ES cell clones was performed by digestion of genomic DNA with AflII (Figure 1A).

Homologous Recombination and Generation of Germline Chimeras

ES cells (RW4, Genome Systems, St. Louis, MO) were electroporated with 10 μg of linearized targeting vector and selected with geneticin (G418, Sigma Chemicals, St. Louis, MO) and 1−[2'-deoxy-2'fluoro-β-D-arabinofuranosyl]-5-iodouracil (FIAU; Bristol-Myers Squibb, Princeton, NJ) (Van Deursen et al., 1995). Three hundred ES colonies doubly resistant to G418 and FIAU were analyzed for homologous recombination using AflII and a 1.0 kb SpeI-ClaI probe (Figure 1A). Four ES clones heterozygous for exon 1β were injected into C57Bl/6 blastocysts, which were subsequently implanted into the uteri of pseudopregnant F1 B/CBA foster mothers and allowed to develop to term. Male chimeras from two clones selected by agouti coat color were mated to C57Bl/6 females. Germline transmission was obtained with one clone. F1 animals were tested for the presence of the deleted *ARF* locus by Southern blotting of tail DNA, and hemizygous F1 males and females were interbred to generate F2 littermates taken for subsequent studies.

Cells and Culture Conditions

Cells were maintained in Dulbecco's modified Eagle's medium (DMEM) supplemented with 10% fetal bovine serum (FBS), 2 mM glutamine, and 100 U/ml penicillin and streptomycin (GIBCO, Grand Island, NY). Balb-3T3 (10)1 and (10)3 derivatives (*INK4a*$^{+}$, *p53*-deleted) were provided by G. Zambetti (St. Jude Children's Research Hospital); mouse erythroleukemia (MEL) cells (*p53*-null, *INK4a*$^{+}$) were from Drs. P. Marks and V. Richon (Memorial Sloan-Kettering Institute, New York, NY). Four previously established MEF cell lines included 5-9, 5-10, 6-14 (*INK4a*$^{+}$, *p53* mutant plus wild type), and 6-18 (*INK4a*$^{-}$, p53 wild type) (Zindy et al., 1997). The 293T retrovirus packaging line and helper virus plasmid (Pear et al., 1993) were obtained from C. Sawyers (University of California, Los Angeles) with permission from David Baltimore (Massachusetts Institute of Technology).

MEFs were derived from 13.5-day-old embryos using a 3T9 protocol based on a strategy of Todaro and Green, 1993. Following removal of the head and organs, embryos were rinsed with phosphate-buffered saline (PBS), minced, and digested with trypsin (0.05% solution containing 0.53 mM EDTA) for 10 min at 37°C, using 1 ml per embryo. Trypsin was inactivated by addition of DMEM containing 10% FBS and 2 mM glutamine, 0.1 mM MEM nonessential amino acids, 55 μM 2-mercaptoethanol, and 10 μg/ml gentamycin. Cells from single embryos were plated into two 60 mm diameter culture dishes and incubated at 37°C in a 10% CO_2 humidified chamber. Cells were maintained on a defined schedule (9×10^5 cells per 60 mm diameter dish passaged every 3 days). Plating after disaggregation of embryo cells was considered passage 1, and the first replating three days later as passage 2. Growth curves at passages 5 and 10 were initiated with replicate cultures of 2×10^4 cells per 60 mm diameter dish; duplicate cultures were counted daily thereafter.

Focus Formation Assay

MEF cells at passages 6 to 8 were seeded at 3×10^5 cells per 35 mm diameter plate and cultured overnight in complete medium containing 10% FBS. Transfections were performed with SuperFect reagents (Qiagen, Santa Clara, CA) per manufacturer's instructions. Expression vector plasmid DNAs, pDCR and pDCR-*ras*V12 (Michael A. White, Southwestern Medical Center, Dallas TX), were mixed with a vector encoding β-galactosidase, and complex formation with SuperFect reagent was performed. After 5 hr of incubation of duplicate cultures with DNA complexes, cells were washed once with PBS and transferred into complete medium containing 10% FBS for 2 days. One plate was used for detection of β-galactosidase-positive cells in order to estimate transfection efficiency. Cells from the other plate were distributed equally into three 60 mm diameter culture dishes, grown in complete medium containing 5% FBS, and refed with fresh medium every 2 days. Twenty-one days post-transfection, cells were fixed and stained with Giemsa. Unfixed foci of morphologically transformed cells were subcloned using microcylinders, expanded, and tested for anchorage-independent growth in 0.3% Noble agar (2×10^4 cells per dish) in Iscove's medium supplemented with 15% FBS, and colonies were scored 2–3 weeks later.

Vector Virus Production and Infection

Human kidney 293T cells were transfected with 15 μg of ecotropic helper virus DNA plasmid plus 15 μg of SRα vector DNA encoding p19^{ARF} (Quelle et al., 1995b). Cell supernatants containing infectious retroviral pseudotypes were harvested 24–60 hr posttransfection, pooled on ice, and filtered (0.45 mm membrane). Infections of exponentially growing mouse fibroblasts were performed in an 8% CO_2 atmosphere with 2 ml of virus-containing culture supernatant containing 10 mg/ml polybrene (Sigma, St. Louis, MO) for each 100 mm diameter plate culture. After 3 hr, 10 ml fresh medium was added. Cells were harvested 48 hr after infection and the percentage in S

phase was determined by flow cytometric analysis of DNA content or by incorporation of [^{3}H]thymidine into replicating cell DNA.

[^{3}H]Thymidine Incorporation into DNA

Cells infected with viral vector plasmids encoding p19^{ARF} or lacking cDNA inserts were distributed at 5×10^3 cells per well into 96-well microtiter plates. Following attachment, the cells were starved in complete medium containing 0.1% FBS and then restimulated with complete serum-containing medium to reenter the cell division cycle. [^{3}H]thymidine (5 Ci/mmol, 0.1 μCi/well; Amersham) was added with the medium, and 24 hr later, incorporation of radioactivity into DNA was measured in disrupted cells trapped on ethanol-washed filters using a Wallac Betaplate scintillation counter (Gaithersburg, MD).

RNA Expression and Nucleotide Sequencing

Total RNA extracted from mouse tissues and pellets of cultured cells was used as a template for cDNA synthesis using a StrataScript RT-PCR kit (Stratagene, La Jolla, CA) per manufacturer's instructions. PCR amplification of transcripts encoding either p16^{INK4a} or p19^{ARF} was performed (Quelle et al., 1995b) using 5′ sense primers based on unique exon 1α or exon 1β sequences and a 3′ antisense primer based on a common exon 2 sequence. RT-PCR products ~0.5 kb in length were detected by direct ethidium bromide staining after electrophoretic separation on agarose gels. DNA sequencing of both strands was performed with the same primers using dideoxynucleotide chain termination and automated fluorescent-based analysis.

Protein Analysis

For analysis of p16^{INK4a} and p19^{ARF} expression, frozen mammalian cell pellets (1×10^7 cells per ml) or tissue samples were disrupted in ice-cold EBC buffer (120 mM NaCl, 50 mM Tris HCl, pH 8.0, 0.5% NP-40, 1 mM EDTA) and left for 1 hr on ice. Nuclei and debris were removed by centrifugation in a microfuge at 12,000 RPM for 10 min at 4°C. Proteins (1 mg/ml) were immunoprecipitated, electrophoretically separated on denaturing polyacrylamide gels containing sodium dodecyl sulfate (SDS), transferred to nitrocellulose, and detected using affinity-purified rabbit antibodies raised to the C-terminal peptides of either p16^{INK4a} or p19^{ARF} (Quelle et al., 1995a, 1995b). Sites of antibody binding were visualized by enhanced chemiluminescence (ECL, Amersham). Where indicated, p16^{INK4a} immunoprecipitates were separated on gels and blotted with rabbit antiserum to CDK4. p21^{Cip1} and p53 were visualized by direct immunoblotting with commercial antibodies (monoclonal F-5 [Santa Cruz Biochemicals] and Ab-7 [Calbiochem, La Jolla CA], respectively).

MEF cells metabolically labeled for 2 hr with 200 mCi/ml [^{35}S]methionine (1369 Ci/mmol, ICN Pharmaceuticals, Costa Mesa, CA) were lysed in 50 mM Tris HCl (pH 8.0), containing 150 mM NaCl, 5 mM EDTA, and 0.5% Nonidet P-40. Centrifuged cell lysates were precipitated using PAb246, a mouse-specific and conformation-dependent antibody that recognizes wild-type but generally not mutant p53 (Yewdell et al., 1986), and PAb240, a panspecific antibody that recognizes many mutant p53s but not the wild-type protein in its native conformation (Gannon et al., 1990). Precipitates were solubilized in gel sample buffer, electrophoretically separated on denaturing polyacrylamide gels, and visualized by autoradiography of the dried slab gels.

Radiation Response

Replicative DNA synthesis was quantitated by bivariate flow cytometry following procedures for irradiation described by others (Deng et al., 1995). In brief, cells made quiescent by serum starvation for 96 hr were irradiated with 5 or 20 Gy and then released into complete medium containing 10% FBS and 65 μM BrdU. Cells were fixed 24 hr later in 70% ethanol and kept at −20°C until analysis. We compared two independently derived *ARF*$^{+/+}$ strains (2 cultures of each) with two *ARF*$^{-/-}$ strains (2 cultures) in two separate experiments. Data for +/+ and −/− strains in each experiment were separately pooled. Fixed cells were incubated in 4N HCl for 30 min at room temperature, washed with PBS, and resuspended in 0.1 M Borax containing 0.1% Tween-30 and 0.1% BSA. Cells were exposed for 30 min at room temperature to monoclonal anti-BrdU (Becton Dickinson, San Jose, CA) or to isotype-matched control mouse immunoglobulin G (IgG), washed with PBS, and counterstained for 30 min with fluorescein-conjugated goat antibodies to mouse IgG (Coulter, Hialeah, FL). Washed cells were resuspended in PBS containing 0.5% BSA, 20 μg/ml propidium iodide, and 50 μg/ml DNAse-free RNAse (Calbiochem), incubated at room temperature for 30 min, and analyzed by flow cytometry. Fluorescence from FITC-labeled incorporated BrdU and propidium iodide-DNA complexes was measured on a FACSCalibur flow cytometer (Becton Dickinson) using 488 nm laser excitation. Cell debris and background artifacts were electronically gated out, and the percentages of cells in different cell cycle phases were computed using CellQuest software (Becton Dickinson). Similar numbers of cells were analyzed for each sample with all standard deviations less than ±4% of the mean.

Acknowledgments

We thank G. Zambetti for monoclonal antibodies to p53, for Balb-3T3 cells lacking p53, and for advice about p53 detection; B. Sorretino and J. Allay for SCID mice; S. van Baal for help with illustrations; C. Naeve for automated sequencing; D. Baltimore and C. Sawyers for 293T cells and helper virus vectors; V. Richon and P. Marks for MEL cells; M. White for the *ras* expression vector; J. van Deursen for critical advice regarding ES cell screening; M. Adachi for help with genomic DNA cloning; and C. Bockhold, C. Nagy, E. Van De Kamp, and J. Watson for technical assistance. This work was supported in part by Cancer Center CORE Grant CA21765, NIH Program Project Grant CA71907, and by ALSAC of St. Jude Children's Research Hospital. C. J. S. dedicates this paper to Drs. George Todaro and Howard Green who taught him about 3T3 cells so long ago that they will no longer remember.

Received September 26, 1997; revised October 16, 1997.

References

Alcorta, D.A., Xiong, Y., Phelps, D., Hannon, G., Beach, D., and Barrett, J.C. (1996). Involvement of the cyclin-dependent kinase inhibitor p16 (INK4a) in replicative senescence of normal human fibroblasts. Proc. Natl. Acad. Sci. USA *93*, 13742–13747.

Deng, C., Zhang, P., Harper, J.W., Elledge, S.J., and Leder, P. (1995). Mice lacking p21$^{CIP1/WAF1}$ undergo normal development, but are defective in G1 checkpoint control. Cell *82*, 675–684.

Donehower, L.A., Harvey, M., Slagle, B.L., McArthur, M.J., Montgomery, C.A., Jr., Butel, J.S., and Bradley, A. (1992). Mice deficient for p53 are developmentally normal but susceptible to spontaneous tumours. Nature *356*, 215–221.

Duro, D., Bernard, O., Della Valle, V., Berger, R., and Larsen, C.-J. (1995). A new type of p16$^{INK4/MTS1}$ gene transcript expressed in B-cell malignancies. Oncogene *11*, 21–29.

El-Deiry, W.S., Tokino, T., Velculescu, V.E., Levy, D.B., Parsons, R., Trent, J.M., Lin, D., Mercer, E., Kinzler, K.W., and Vogelstein, B. (1993). WAF1, a potential mediator of p53 tumor suppression. Cell *75*, 817–825.

Fitzgerald, M.G., Harkin, D.P., Silva-Arrieta, S., MacDonald, D.J., Lucchina, L.C., Unsal, H., O'Neill, E., Koh, J., Finkelstein, D.M., Isselbacher, K.J., et al. (1996). Prevalence of germ-line mutations in p16, p19^{ARF}, and CDK4 in familial melanoma: analysis of a clinic-based population. Proc. Natl. Acad. Sci. USA *93*, 8541–8545.

Fukusawa, K., Choi, T., Kuriyama, R., Rulong, S., and Vande Woude, G.F. (1996) Abnormal centrosome amplification in the absence of p53. Science *271*, 1744–1747.

Gannon, J.V., Greaves, R., Iggo, R., and Lane, D.P. (1990). Activating mutations in p53 produce a common conformational effect: a monoclonal antibody specific for the mutant form. EMBO J. *9*, 1595–1602.

Gottlieb, T.M., and Oren, M. (1996). p53 in growth control and neoplasia. Biochim. Biophys. Acta *1287*, 77–102.

Gruis, N.A., van der Velden, P.A., Sandkuijl, L.A., Prins, D.E., Weaver-Feldhaus, J., Kamb, A., Bergman, W., and Frants, R. (1995). Homozygotes for CDKN2 (p16) germline mutation in Dutch familial melanoma kindreds. Nature Genet. *10*, 351–353.

Hainaut, P., Soussi, T., Shomer, B., Hollstein, M., Greenblatt, M., Hovig, E., Harris, C.C., and Montesano, R. (1997). Database of p53 gene somatic mutations in human tumors and cell lines: updated compilation and future prospects. Nucleic Acids Res. *25*, 151–157.

Hall, M., and Peters, G. (1996). Genetic alterations of cyclins, cyclin-dependent kinases, and cdk inhibitors in human cancer. Adv. Cancer Res. *68*, 67–108.

Hara, E., Smith, R., Parry, D., Tahara, H., Stone, S., and Peters, G. (1996). Regulation of $p16^{CDKN2}$ expression and its implications for cell immortalization and senescence. Mol. Cell. Biol. *16*, 859–867.

Harvey, D.M., and Levine, A.J. (1991). p53 alteration is a common event in the spontaneous immortalization of primary BALB/c murine embryo fibroblasts. Genes Dev. *5*, 2375–2385.

Harvey, M., Sands, A.T., Weiss, R.S., Hegi, M.E., Wiseman, R.W., Pantazis, P., Giovanella, B.C., Tainsky, M.A., Bradley, A., and Donehower, L.A. (1993). In vitro growth characteristics of embryo fibroblasts isolated from p53-deficient mice. Oncogene *8*, 2457–2467.

Herzog, C.R., Soloff, E.V., Mcdoniels, A.L., Tyson, F.L., Malkinson, A.M., Haugen-Strano, A., Wiseman, R.W., Anderson, M.W., and You, M. (1996). Homozygous codeletion and differential decreased expression of $p15^{INK4b}$, $p16^{INK4a}$-α, and $p16^{INK4a}$-β in mouse lung tumor cells. Oncogene *13*, 1885–1891.

Hirama, T. and Koeffler, H.P. (1995). Role of cyclin-dependent kinase inhibitors in the development of cancer. Blood *86*, 841–854.

Holland, E.A., Beaton, S.C., Becker, T.M., Grulet, O.M.C., Peters, B.A., Rizos, H., Kefford, R.F., and Mann, G.J. (1995). Analysis of the p16 gene, CDKN2, in 17 Australian melanoma kindreds. Oncogene *11*, 2289–2294.

Hunter, T. and Pines, J. (1994). Cyclins and cancer II: cyclin D and CDK inhibitors come of age. Cell *79*, 573–582.

Jacks, T., Remington, L., Williams, B.O., Schmitt, E.M., Halachmi, S., Bronson, R.T., and Weinberg, R.A. (1994). Tumor spectrum analysis in p53-mutant mice. Curr. Biol. *4*, 1–7.

Kamb, A., Gruis, N.A., Weaver-Feldhaus, J., Liu, Q., Harshman, K., Tavtigian, S.V., Stockert, E., Day, R.S., III., Johnson, B.E., and Skolnick, M.H. (1994). A cell cycle regulator involved in genesis of many tumor types. Science *264*, 436–440.

Kastan, M.B., Onyekwere, O., Sidransky, D., Vogelstein, B., and Craig, R.W. (1991). Participation of p53 protein in the cellular response to DNA damage. Cancer Res. *51*, 6304–6311.

Kemp, C.J., Wheldon, T., and Balmain, A. (1994) p53-deficient mice are extremely susceptible to radiation-induced tumorigenesis. Nature Genet. *8*, 66–69.

Ko, L.J. and Prives, C. (1996). p53: puzzle and paradigm. Genes Dev. *10*, 1054–1072.

Koh, J., Enders, G.H., Dynlacht, B.D., and Harlow, E. (1995). Tumour-derived p16 alleles encoding proteins defective in cell cycle inhibition. Nature *375*, 506–510.

Kubo, Y., Urano, Y., Matsumoto, K., Ahsan, K., and Arase, S. (1997). Mutations of the INK4a locus in squamous cell carcinomas of human skin. Biochem. Biophys. Res. Commun. *232*, 38–41.

Kuerbitz, S.J., Plunkett, B.S., Walsh, W.V., and Kastan, M.B. (1992). Wild-type p53 is a cell cycle checkpoint determinant following irradiation. Proc. Nat. Acad. Sci. USA *89*, 7491–7495.

Levine, A.J. (1997). p53, the cellular gatekeeper for growth and division. Cell *88*, 323–331.

Lloyd, A.C., Obermuller, F., Staddon, S., Barth, C.F., McMahon, M., and Land, H. (1997). Cooperating oncogenes converge to regulate cyclin/cdk complexes. Genes Dev. *11*, 663–667.

Lukas, J., Parry, D., Aagaard, L., Mann, D.J., Bartkova, J., Strauss, M., Peters, G., and Bartek, J. (1995). Retinoblastoma protein-dependent cell cycle inhibition by the tumor suppressor p16. Nature *375*, 503–506.

Mao, L., Merlo, A., Bedi, G., Shapiro, G.I., Edwards, C.D., Rollins, B.J., and Sidransky, D. (1995). A novel $p16^{INK4a}$ transcript. Cancer Res. *55*, 2995–2997.

Merlo, A., Herman, J.G., Mao, L., Lee, D.J., Gabrielson, E., Burger, P.C., Baylin, S.B., and Sidransky, D. (1995). 5′ CpG island methylation is associated with transcriptional silencing of the tumour suppressor p16/CDKN2/MTS1 in human cancers. Nature Med. *1*, 686–692.

Naito, M. and DiGiovanni, J. (1989). Genetic background and development of skin tumors. In Carcinogenesis, Vol.III, Skin Tumors: Experimental and Clinical Aspects. C.J. Conti, T.J. Slaga, and A.J.P. Klein-Szanto, eds. (New York: Raven Press), pp. 187–212.

Noble, J.R., Rogan, E.M., Neumann, A.A., Maclean, K., Bryan, T.M., and Reddel, R.R. (1996). Association of extended *in vitro* proliferative potential with loss of $p16^{INK4}$ expression. Oncogene *13*, 1259–1268.

Nobori, T., Miura, K., Wu, D.J., Lois, A., Takabayashi, K., and Carson, D.A. (1994). Deletions of the cyclin-dependent kinase-4 inhibitor gene in multiple human cancers. Nature *368*, 753–756.

Noda, A., Ning, Y., Venable, S.F., Pereira-Smith, O.M., and Smith, J.R. (1994). Cloning of senescent cell-derived inhibitors of DNA synthesis using an expression screen. Exp. Cell Res. *211*, 90–98.

Parry, D. and Peters, G. (1996). Temperature-sensitive mutants of $p16^{CDKN2}$ associated with familial melanoma. Mol. Cell. Biol. *16*, 3844–3852.

Pear, W.S., Nolan, G.P., Martin, L.S., and Baltimore, D. (1993). Production of higher-titer helper-free retroviruses by transient transfection. Proc. Natl. Acad. Sci. USA *90*, 8392–8396.

Pollock, P.M., Pearson, J.V., and Hayward, N.K. (1996). Compilation of somatic mutations of the CDKN2 gene in human cancers: nonrandom distribution of base substitutions. Genes Chrom. Cancer *15*, 77–88.

Quelle, D.E., Ashmun, R.A., Hannon, G.J., Rehberger, P.A., Trono, D., Richter, K.H., Walker, C., Beach, D., Sherr, C.J., and Serrano, M. (1995a). Cloning and characterization of murine $p16^{INK4a}$ and $p15^{INK4b}$ genes. Oncogene *11*, 635–645.

Quelle, D.E., Zindy, F., Ashmun, R.A., and Sherr, C.J. (1995b). Alternative reading frames of the INK4a tumor suppressor gene encode two unrelated proteins capable of inducing cell cycle arrest. Cell *83*, 993–1000.

Quelle, D.E., Cheng, M., Ashmun, R.A., and Sherr, C.J. (1997). Cancer-associated mutations at the *INK4a* locus cancel cell cycle arrest by $p16^{INK4a}$ but not by the alternative reading frame protein $p19^{ARF}$. Proc. Natl. Acad. Sci. USA *94*, 3436–3440.

Ranade, K., Hussussian, C.J., Sikorski, R.S., Varmus, H.E., Goldstein, A.M., Tucker, M.A., Serrano, M., Hannon, G.J., Beach, D., and Dracopoli, N.C. (1995). Mutations associated with familial melanoma impair p16INK4 function. Nature Genetics *10*, 114–116.

Reiners, J.J., Jr., Nesnow, S., and Slaga, T.J. (1984). Murine susceptibility to two-stage skin carcinogenesis is influenced by the agent used for promotion. Carcinogenesis *5*, 301–307.

Reymond, A., and Brent, R. (1995). p16 proteins from melanoma-prone families are deficient in binding to Cdk4. Oncogene *11*, 1173–1178.

Reznikoff, C.A., Yeager, T.R., Belair, C.D., Savelieva, E., Puthenveettil, J.A., and Stadler, W.M. (1996). Elevated p16 at senescence and loss of p16 at immortalization in human papillomavirus 16 E6, but not E7, transformed human uroepithelial cells. Cancer Res. *56*, 2886–2890.

Rittling, S.R. and Denhardt, D.T. (1992). p53 mutations in spontaneously immortalized 3T12 but not 3T3 mouse embryo cells. Oncogene *7*, 935–942.

Rogan, E.M., Bryan, T.M., Hukku, B., Maclean, K., Chang, A.C.M., Moy, E.L., Englezou, A., Warneford, S.G., Dalla-Pozza, L., and Reddel, R.R. (1995). Alterations in p53 and $p16^{INK4}$ expression and telomere length during spontaneous immortalization of Li-Fraumeni syndrome fibroblasts. Mol. Cell. Biol. *15*, 4745–4753.

Serrano, M., Hannon, G.J., and Beach, D. (1993). A new regulatory motif in cell cycle control causing specific inhibition of cyclin D/CDK4. Nature *366*, 704–707.

Serrano, M., Lee, H.-W., Chin, L., Cordon-Cardo, C., Beach, D., and DePinho, R.A. (1996). Role of the INK4a locus in tumor suppression and cell mortality. Cell *85*, 27–37.

Serrano, M., Lin, A.W., McCurrach, M.E., Beach, D., and Lowe, S.W. (1997). Oncogenic *ras* provokes premature cell senescence associated with accumulation of p53 and $p16^{INK4a}$. Cell *88*, 593–602.

Shapiro, G.I., Park, J.E., Edwards, C.D., Mao, L., Merlo, A., Sidranski, D., Ewen, M.E., and Rollins, B.J. (1995). Multiple mechanisms of $p16^{INK4a}$ inactivation in non-small cell lung cancer cell lines. Cancer Res. *55*, 6200–6209.

Sherr, C.J. (1996). Cancer cell cycles. Science *274*, 1672–1677.

Stone, S., Jiang, P., Dayananth, P., Tavtigian, S.V., Katcher, H., Parry, D., Peters, G., and Kamb, A. (1995). Complex structure and regulation of the *p16(MTS1)* locus. Cancer Res. *55*, 2988–2994.

Swafford, D.S., Middleton, S.K., Palmisano, W.A., Nikula, K.J., Tesfaigzi, J., Baylin, S.B., Herman, J.G., and Belinsky, S.A. (1997). Frequent aberrant methylation of $p16^{INK4a}$ in primary rat lung tumors. Mol. Cell. Biol. *17*, 1366–1374.

Tanaka, H., Shimada, Y., Imamura, M., Shibagaki, I., and Ishizaki, K. (1997). Multiple types of aberrations in the p16(INK4a) and the p15(INK4b) genes in 30 esophageal squamous-cell-carcinoma cell lines. Int. J. Cancer *70*, 437–442.

Todaro, G.J. and Green, H. (1963). Quantitative studies of the growth of mouse embryo cells in culture and their development into established lines. J. Cell Biol. *17*, 299–313.

Van Deursen, J., Fornerod, M., Van Rees, B., and Grosveld, G. (1995). Cre-mediated site-specific translocation between nonhomologous mouse chromosomes. Proc. Natl. Acad. Sci. USA *92*, 7376–7380.

Walker, G.J., Hussussian, G.J., Flores, J.F., Glendening, J.M., Haluska, F.G., Dracopoli, N.C., Hayward, N.K., and Fountain, J.W. (1995). Mutations of the CDKN2/$p16^{INK4}$ gene in Australian melanoma kindreds. Hum. Mol. Genet. *4*, 1845–1852.

Weinberg, R.A. (1995). The retinoblastoma protein and cell cycle control. Cell *81*, 323–330.

Weinberg, R.A. (1997). The cat and mouse games that genes, viruses, and cells play. Cell *88*, 573–575.

Wick, S.T., Dubay, M.M., Imanil, I., and Brizuela, L. (1995). Biochemical and mutagenic analysis of the melanoma tumor suppressor gene product p16. Oncogene *11*, 2013–2019.

Yang, R.A., Gombart, A.F., Serrano, M., and Koeffler, H.P. (1995). Mutational effects on the p16Ink4a tumor suppressor protein. Cancer Res. *55*, 2503–2506.

Yewdell, J.W., Gannon, J.V., and Lane, D.P. (1986). Monoclonal antibody analysis of p53 expression in normal and transformed cells. J. Virol. *59*, 444–452.

Zindy, F., Quelle, D.E., Roussel, M.F., and Sherr, C.J. (1997). Expression of the $p16^{INK4a}$ tumor suppressor versus other INK4 family members during mouse development and aging. Oncogene *15*, 203–211.